Deep learning approaches to Parkinson's disease markers discovery

Virgilio Kmetzsch

Master of Science in Informatics at Grenoble
Specialization Data Science

June 24, 2019

Outline

Table of Contents

Medical context

Parkinson's disease (PD)

- Neurodegenerative disorder that affects movement

Medical context

Parkinson's disease (PD)

- Neurodegenerative disorder that affects movement

Magnetic Resonance Imaging (MRI)

- Non-invasive medical imaging technique

Medical context

Parkinson's disease (PD)

- Neurodegenerative disorder that affects movement

Magnetic Resonance Imaging (MRI)

- Non-invasive medical imaging technique

Quest of **neuroimaging markers** for Parkinson's early detection

Scientific context

Neuroimaging markers of PD

- Various studies [Peran et al., 2010, Du et al., 2011, Schwarz et al., 2013, Atkinson-Clement et al., 2017]
- Standard statistical methods, e.g. two-sample t-tests
- Inconsistent findings [Schwarz et al., 2013, Atkinson-Clement et al., 2017]

Scientific context

Neuroimaging markers of PD

- Various studies [Peran et al., 2010, Du et al., 2011, Schwarz et al., 2013, Atkinson-Clement et al., 2017]
- Standard statistical methods, e.g. two-sample t-tests
- Inconsistent findings [Schwarz et al., 2013, Atkinson-Clement et al., 2017]

Deep learning

- Increasing interest in medical imaging applications
- Growth in anomaly detection
  [Schlegl et al., 2017, Alex et al., 2017, Baur et al., 2018, Chen and Konukoglu, 2018, Zimmerer et al., 2018, Vu et al., 2019]

Scientific context

Neuroimaging markers of PD

- Various studies [Peran et al., 2010, Du et al., 2011, Schwarz et al., 2013, Atkinson-Clement et al., 2017]
- Standard statistical methods, e.g. two-sample t-tests
- Inconsistent findings [Schwarz et al., 2013, Atkinson-Clement et al., 2017]

Deep learning

- Increasing interest in medical imaging applications
- Growth in anomaly detection
  [Schlegl et al., 2017, Alex et al., 2017, Baur et al., 2018, Chen and Konukoglu, 2018, Zimmerer et al., 2018, Vu et al., 2019]

Bring **together** these two lines of research

Problem statement

- Anomaly detection in multimodal MRI data
  - Reference model trained with MRI from healthy individuals
  - Anomaly detection scheme to identify abnormal patterns

Problem statement

- Anomaly detection in multimodal MRI data
  - Reference model trained with MRI from healthy individuals
  - Anomaly detection scheme to identify abnormal patterns

Can deep learning provide a representation of MRI data from healthy brains and identify PD anomalies?

Problem statement

- Anomaly detection in multimodal MRI data
  - Reference model trained with MRI from healthy individuals
  - Anomaly detection scheme to identify abnormal patterns

Can deep learning provide a representation of MRI data from healthy brains and identify PD anomalies?

Challenges:

1. Limited training data (57 healthy controls)

Problem statement

- Anomaly detection in multimodal MRI data
  - Reference model trained with MRI from healthy individuals
  - Anomaly detection scheme to identify abnormal patterns

Can deep learning provide a representation of MRI data from healthy brains and identify PD anomalies?

Challenges:

1. Limited training data (57 healthy controls)
2. No ground truth at the voxel level

Problem statement

- Anomaly detection in multimodal MRI data
  - Reference model trained with MRI from healthy individuals
  - Anomaly detection scheme to identify abnormal patterns

Can deep learning provide a representation of MRI data from healthy brains and identify PD anomalies?

Challenges:

1. Limited training data (57 healthy controls)
2. No ground truth at the voxel level
3. PD anomalies may be very local

Problem statement

- Anomaly detection in multimodal MRI data
  - Reference model trained with MRI from healthy individuals
  - Anomaly detection scheme to identify abnormal patterns

Can deep learning provide a representation of MRI data from healthy brains and identify PD anomalies?

Challenges:

1. Limited training data (57 healthy controls)
2. No ground truth at the voxel level
3. PD anomalies may be very local
4. Only two quantitative MRI measures are available: fractional anisotropy (FA) and mean diffusivity (MD)

Table of Contents

Autoencoder (AE)

- Objective: learn compressed representations
- Neural network where the output approximates the input
  - Encoder: input data x to latent code z
  - Decoder: latent code z to output $\hat{x}$ (input reconstruction)

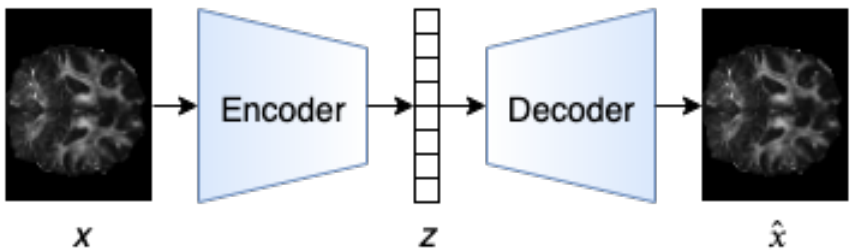

Autoencoder (AE)

- Objective: learn compressed representations
- Neural network where the output approximates the input
  - Encoder: input data x to latent code z
  - Decoder: latent code z to output $\hat{x}$ (input reconstruction)

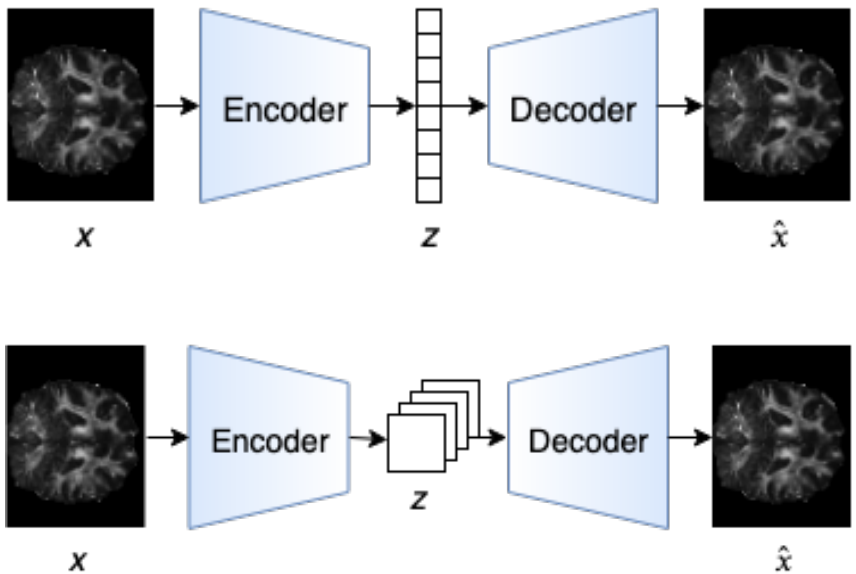

Figure 1: Autoencoders with a dense and spatial bottleneck

Variational autoencoder (VAE) [Kingma and Welling, 2013]

- Based on autoencoders
- Objective: learn distribution $p(x)$ using a latent representation model
- Generative model that can be sampled

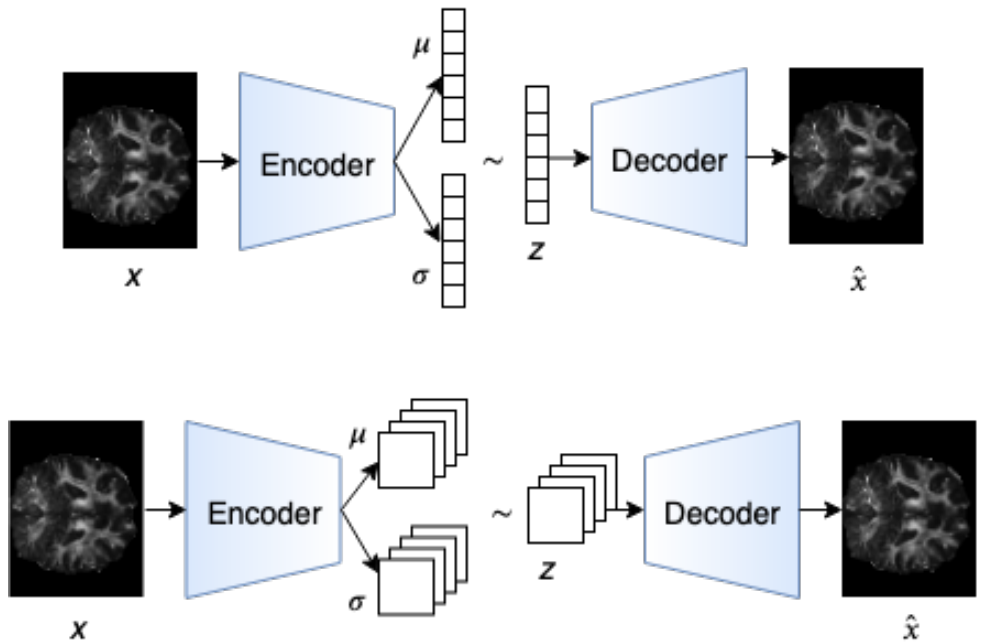

Figure 2: Variational autoencoders with a dense (top) and a spatial (bottom) bottleneck

U-Net [Ronneberger et al., 2015]

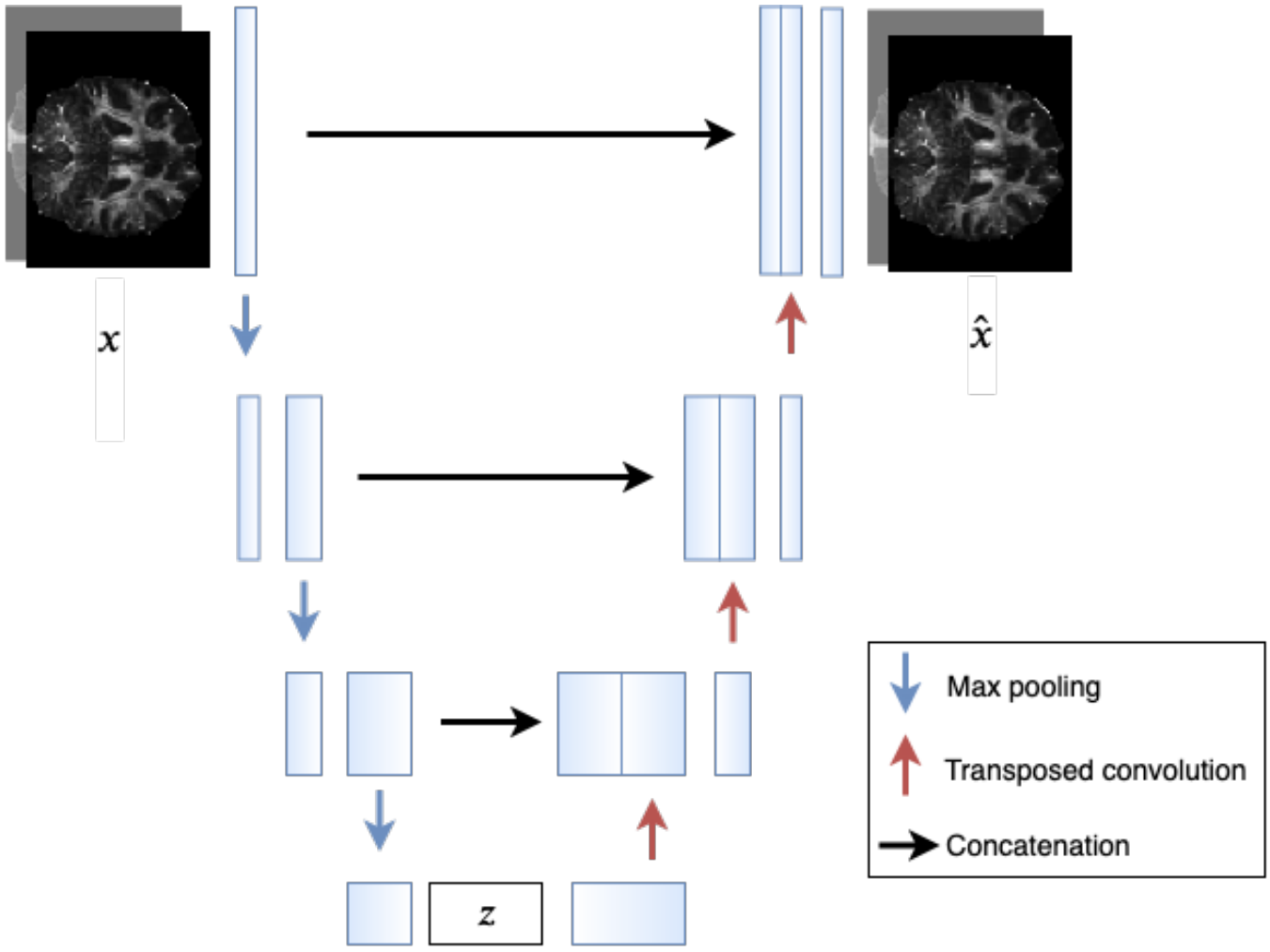

Figure 3: U-Net architecture

- Contracting path, bottleneck, expansive path

Table of Contents

Deep learning for anomaly detection in medical images

- Most frameworks:
  - Use AE, VAE, generative adversarial networks (GAN) [Goodfellow et al., 2014] or combinations
  - Detect lesions visible by humans
  - Perform downsampling
  - Leverage voxel-level ground truth to perform post-processing

Deep learning for anomaly detection in medical images

Our main inspiration was [Baur et al., 2018]

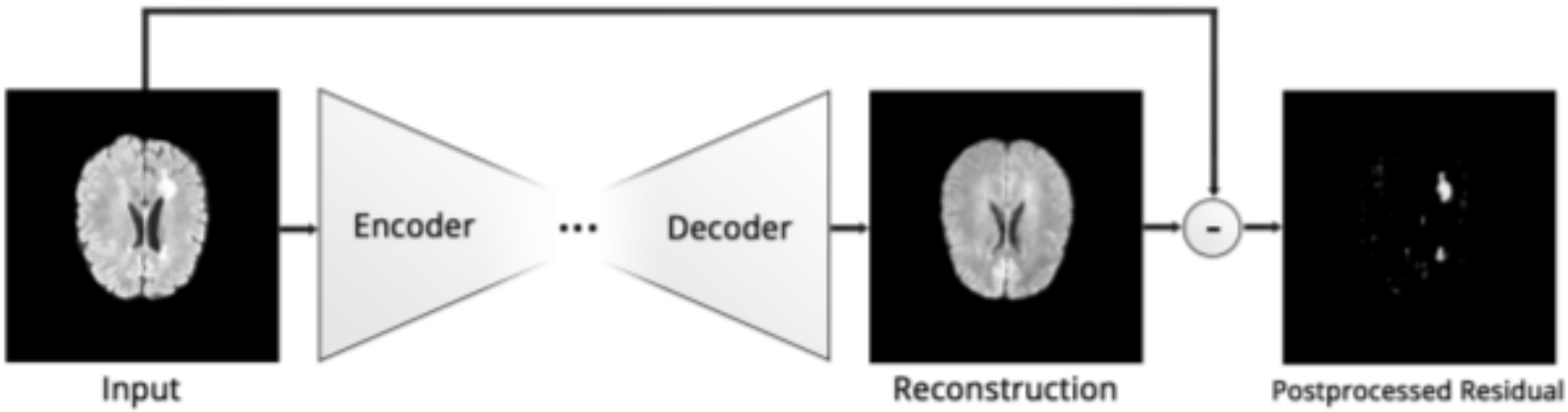

Figure 4: Anomaly detection with reconstruction error. Image from [Baur et al., 2018]

- Train model to capture normal anatomical appearance
- Detected anomalies from poor reconstruction of input

Table of Contents

Data description

- 57 healthy controls and 129 recently diagnosed PD patients

Data description

- 57 healthy controls and 129 recently diagnosed PD patients
- Each MRI volume:
  - 116 x 116 x 72 voxels
  - 2 measures per voxel: FA and MD

Data description

- 57 healthy controls and 129 recently diagnosed PD patients
- Each MRI volume:
  - 116 x 116 x 72 voxels
  - 2 measures per voxel: FA and MD
- 55 entire axial slices of 116 x 72 around the midline
- No downsampling: input, output are third-order tensors:

$$x, \hat{x} \in \mathbb{R}^{116 \times 72 \times 2}$$

Approach

- Unsupervised training with MRI from healthy controls
  - Modeling process: 7-fold cross-validation with 42 controls
  - Final evaluation: train with 42 controls, test with 15 controls
- Four models developed and evaluated
- Reconstruction errors:

$$abs(x - \hat{x})$$

Spatial autoencoder (sAE)

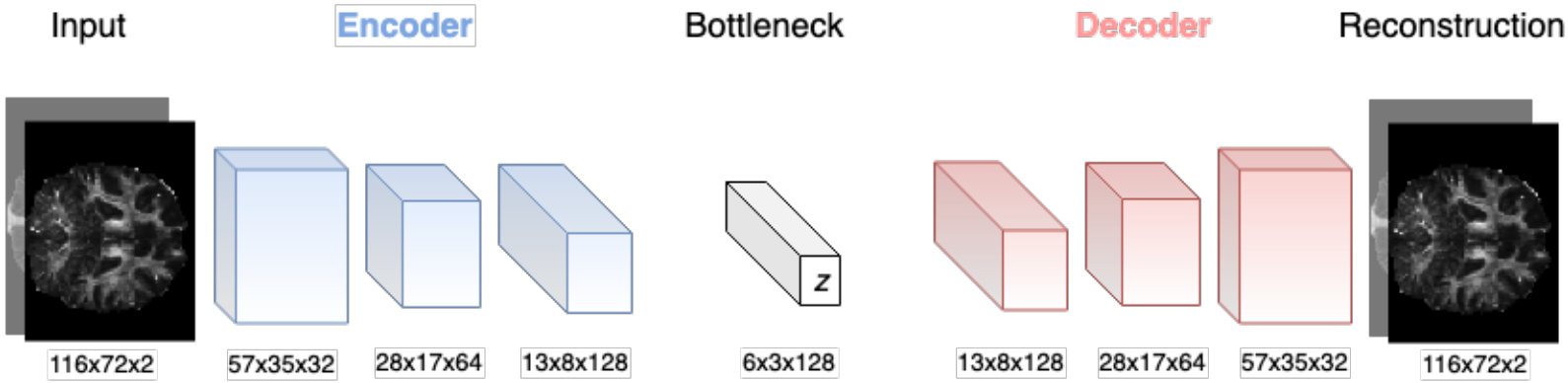

Figure 5: Spatial autoencoder architecture

- Fully convolutional, 5 x 5 kernel, stride of (2, 2)
- 4 convolutional layers from input to bottleneck
- 4 transposed convolutional layers from bottleneck to output
- $\mathcal{L} = \|x - \hat{x}\|_1$

Spatial variational autoencoder (sVAE)

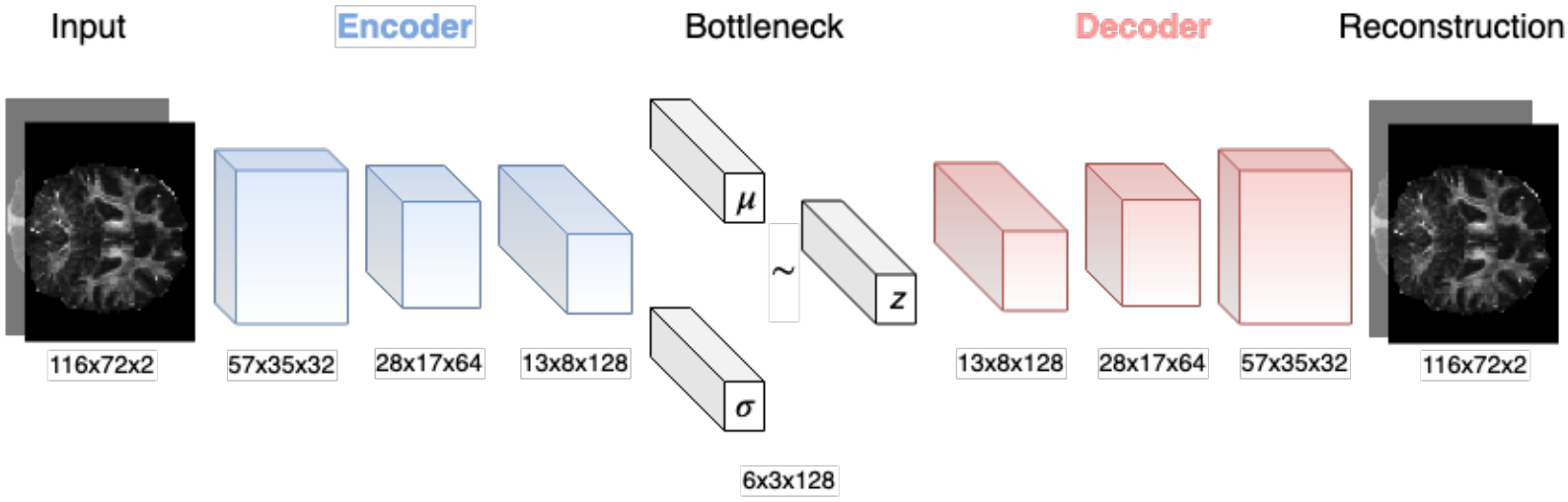

Figure 6: Spatial variational autoencoder architecture

- Fully convolutional, 5 x 5 kernel, stride of (2, 2)
- 4 convolutional layers from input to bottleneck
- 4 transposed convolutional layers from bottleneck to output
- $\mathcal{L} = \lambda \underbrace{\|x - \hat{x}\|_1}_{\text{Rec. error}} + (1-\lambda) \underbrace{\left[-\frac{1}{2} \sum_{j=1}^{J} (1 + \log((\sigma_j)^2) - (\mu_j)^2 - (\sigma_j)^2) \right]}_{D_{KL}[q_\phi(z|x)||p(z)] \text{ for Gaussian case}^1}$

[1] [Kingma and Welling, 2013]

Dense variational autoencoder (dVAE)

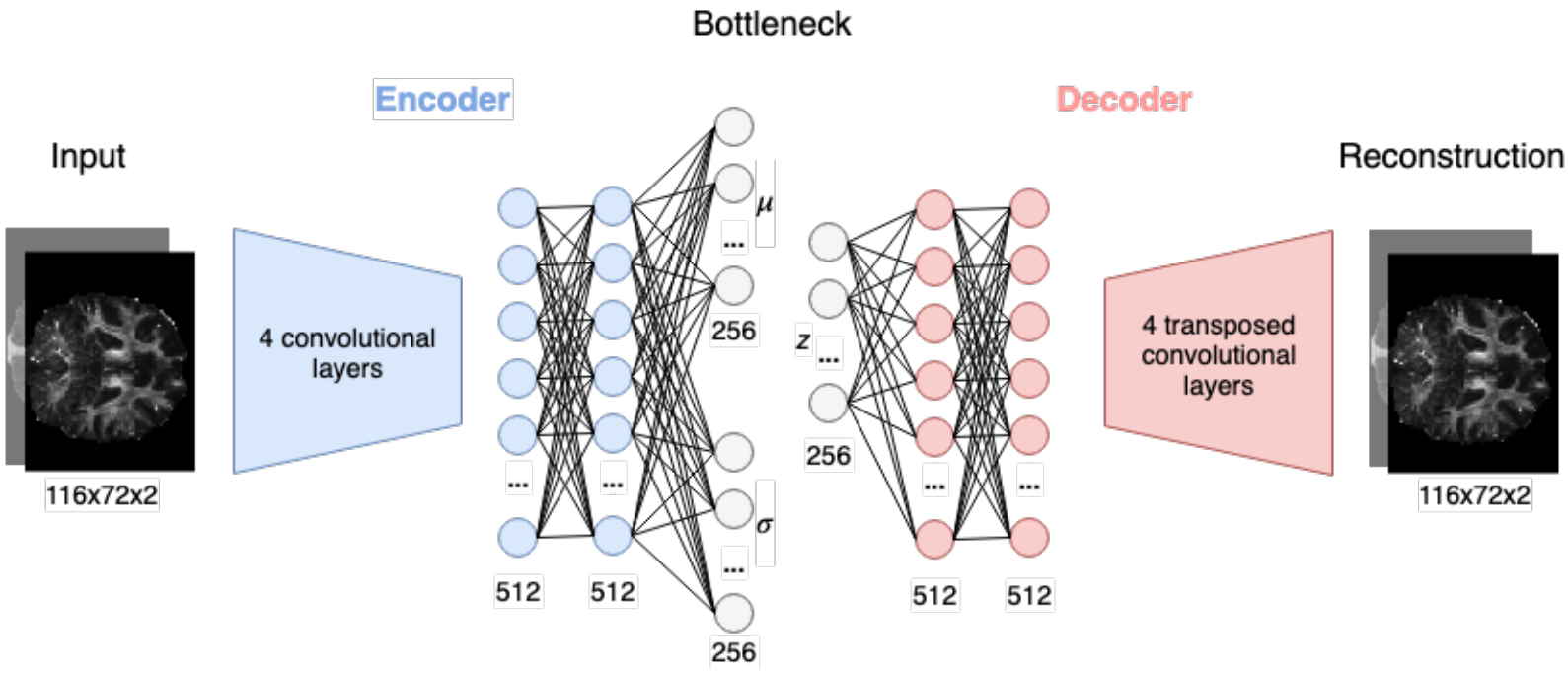

Figure 7: Dense variational autoencoder architecture

- Convolutional layers: 5 x 5 kernel, stride of (2, 2)
- 3 fully connected layers in the encoder and 3 in the decoder
- $\mathcal{L} = \lambda \underbrace{\|x - \hat{x}\|_1}_{\text{Rec. error}} + (1-\lambda) \underbrace{\left[-\frac{1}{2} \sum_{j=1}^{J} (1 + \log((\sigma_j)^2) - (\mu_j)^2 - (\sigma_j)^2) \right]}_{D_{KL}[q_\phi(z|x)||p(z)] \text{ for Gaussian case}^2}$

[2] [Kingma and Welling, 2013]

U-Net

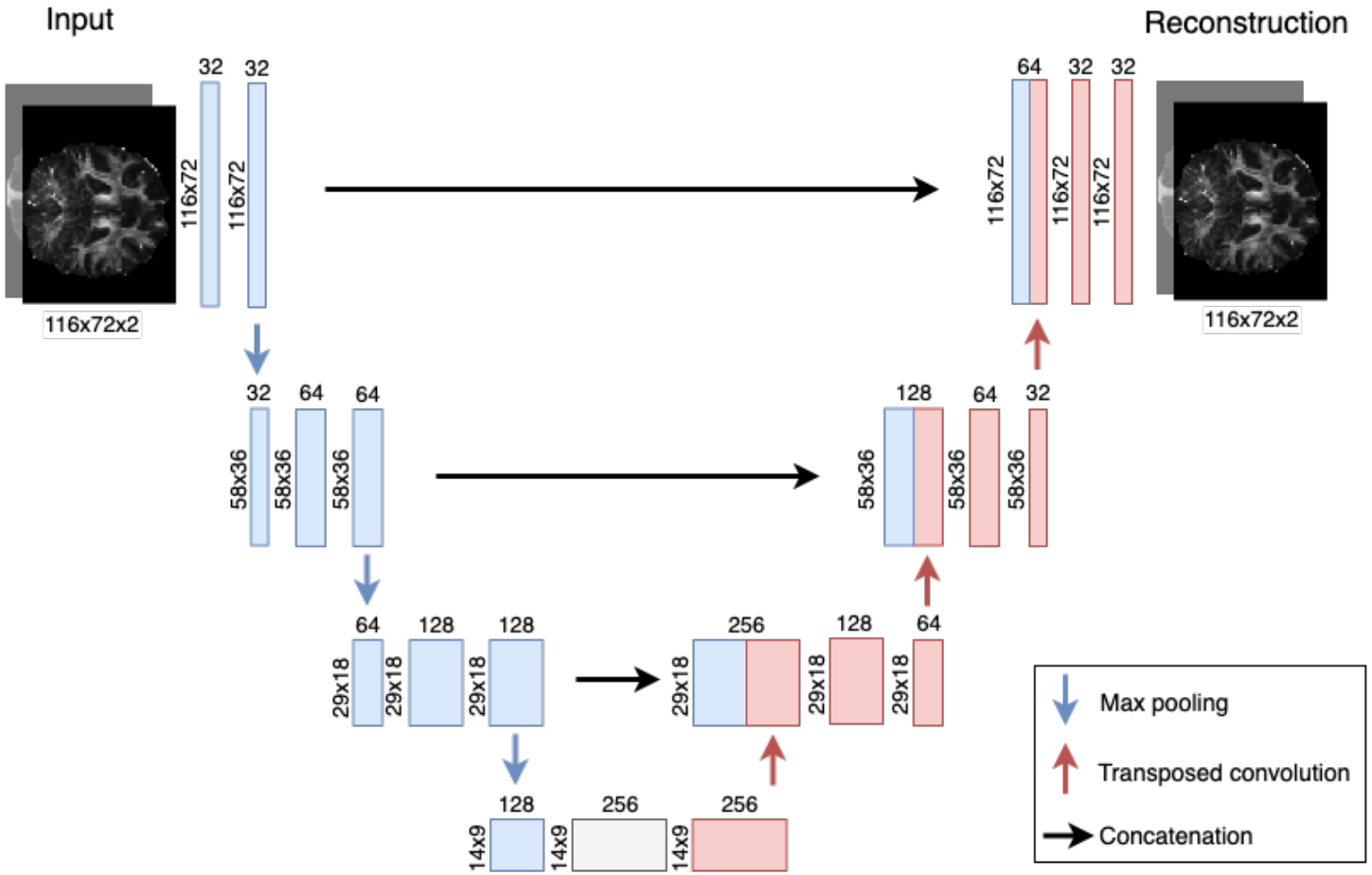

Figure 8: U-Net architecture

- 3 x 3 kernel, stride of (1, 1) in convolutions, stride of (2, 2) in transposed convolutions
- $\mathcal{L} = \|x - \hat{x}\|_1$

Table of Contents

Reconstructions

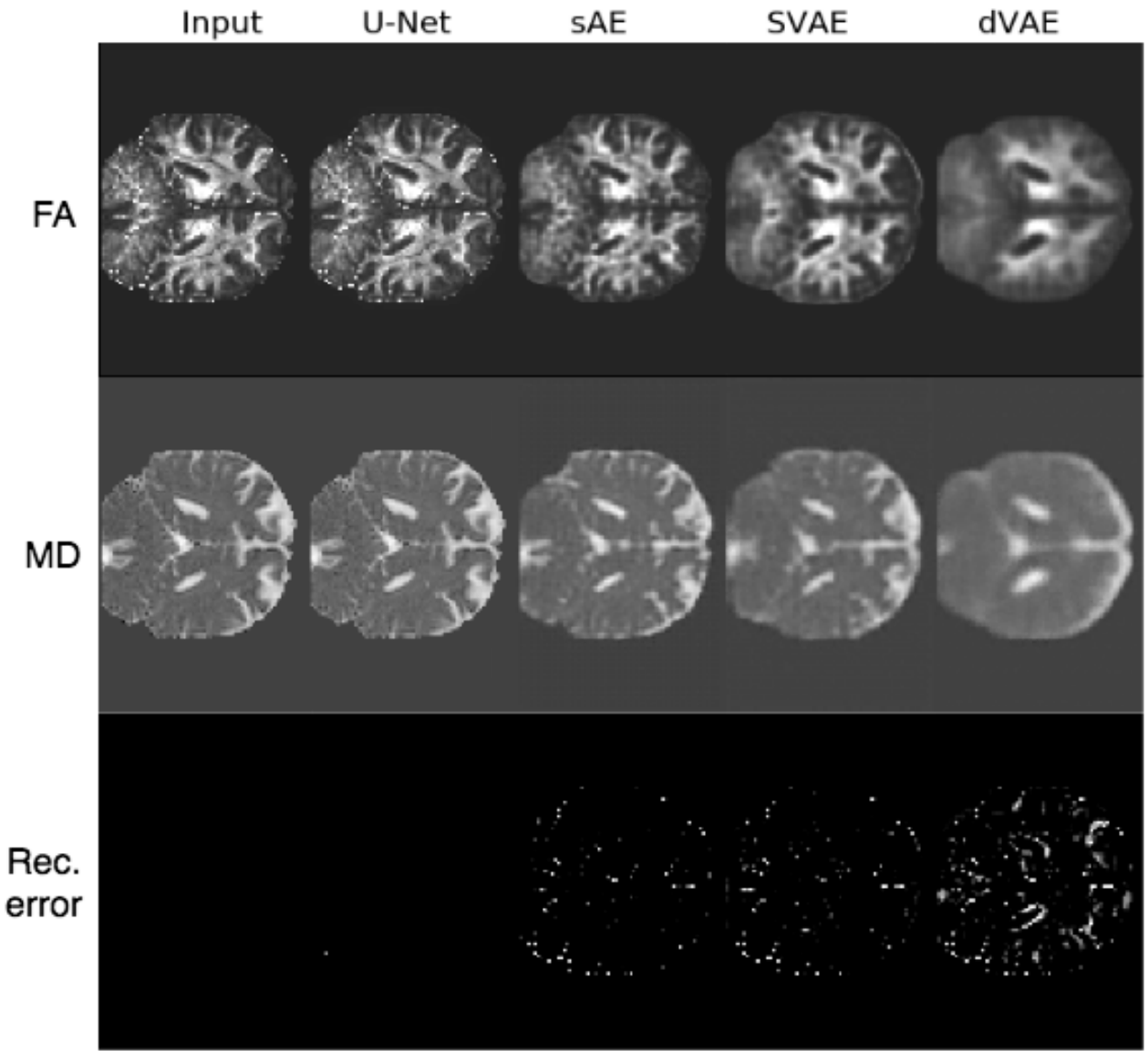

Figure 9: Randomly selected patient, slice 19

Reconstructions

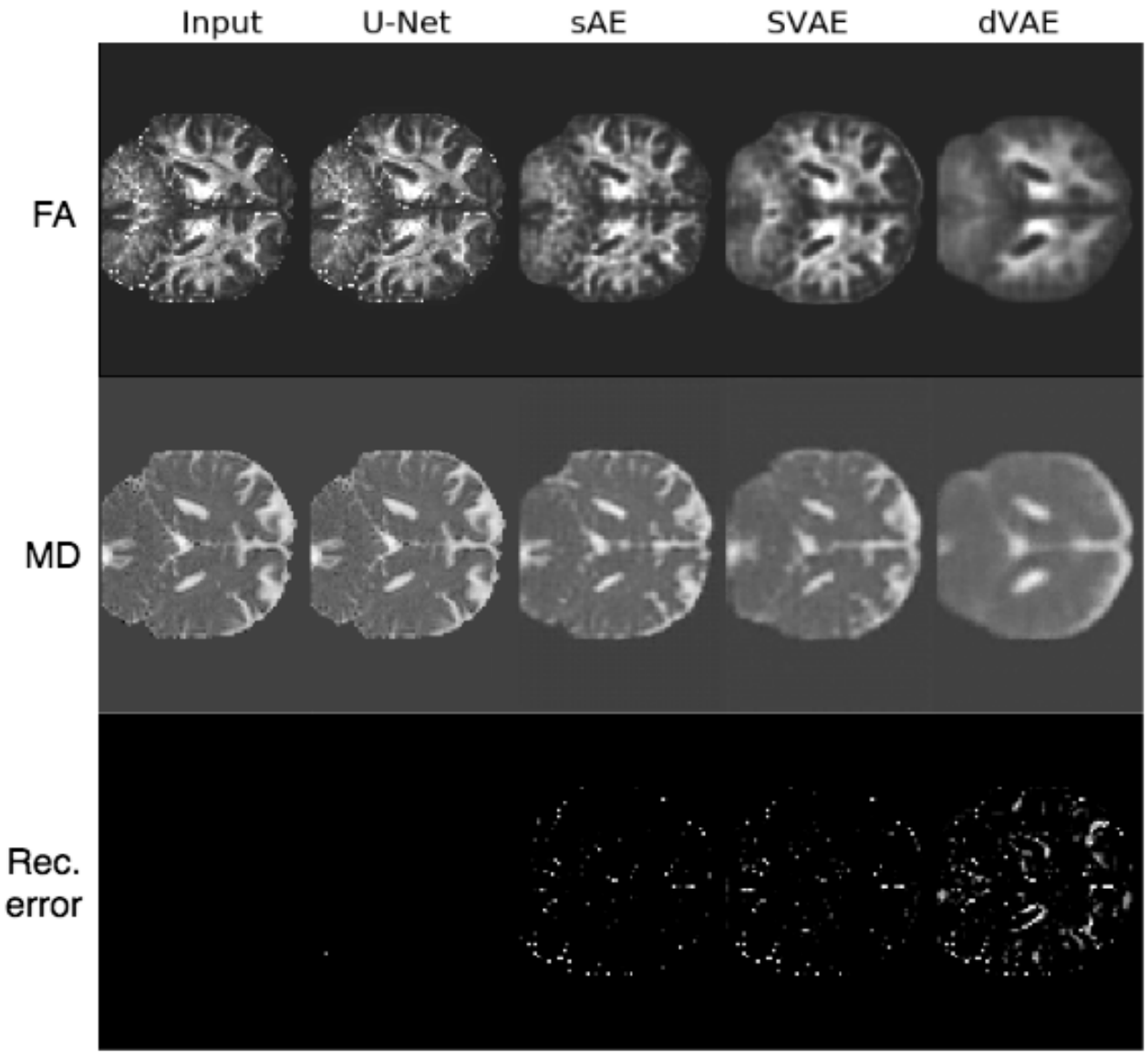

Figure 9: Randomly selected patient, slice 19

- Noise in the input data
- Compressed representation
- Variability of healthy individuals
- **Real PD anomalies**

Regions of Interest (ROI)

8 regions

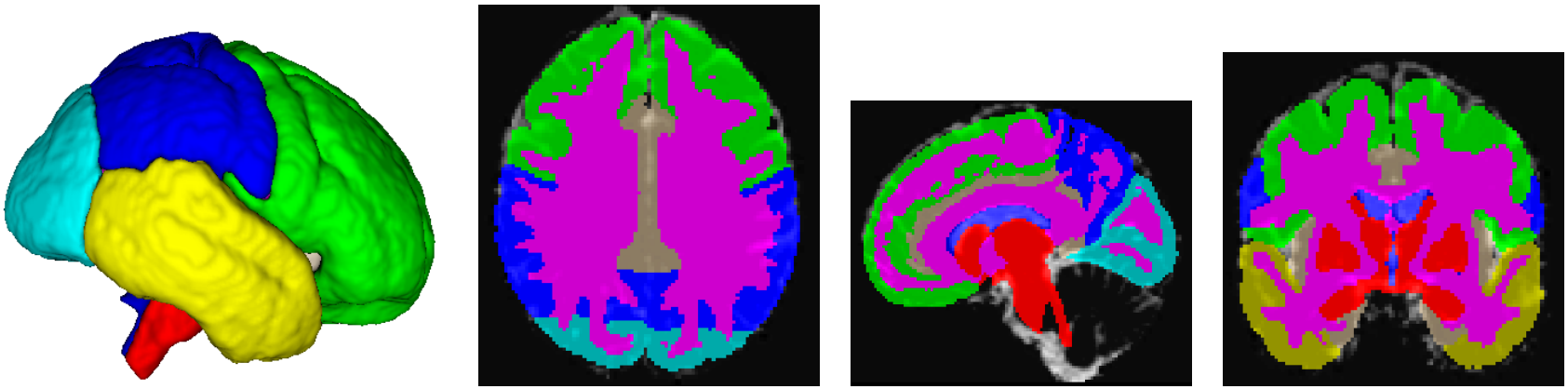

Figure 10: 3D representation, axial slice, sagittal slice and coronal slice depicting 8 brain regions

Regions of Interest (ROI)

8 regions

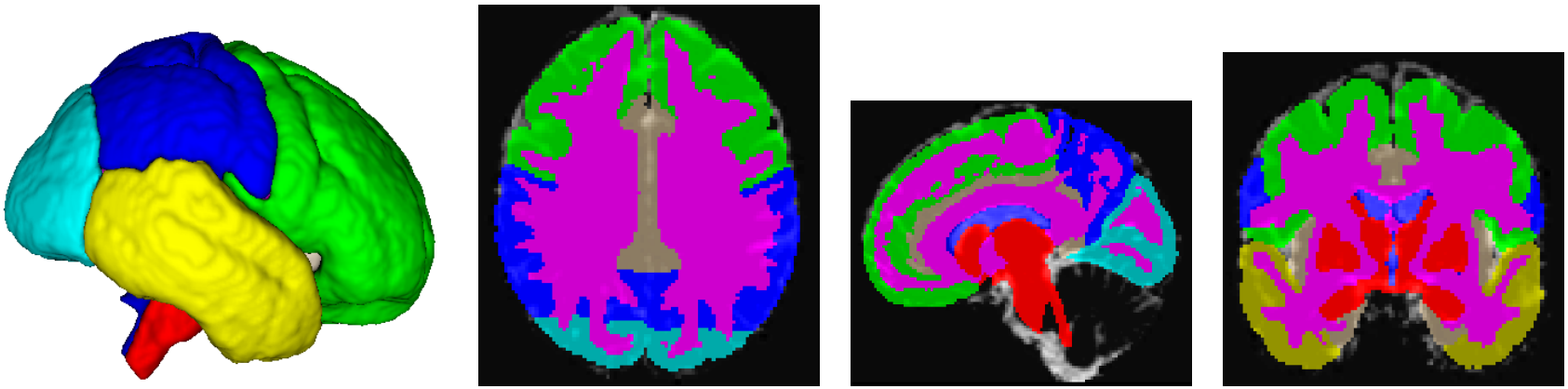

Figure 10: 3D representation, axial slice, sagittal slice and coronal slice depicting 8 brain regions

10 subcortical structures

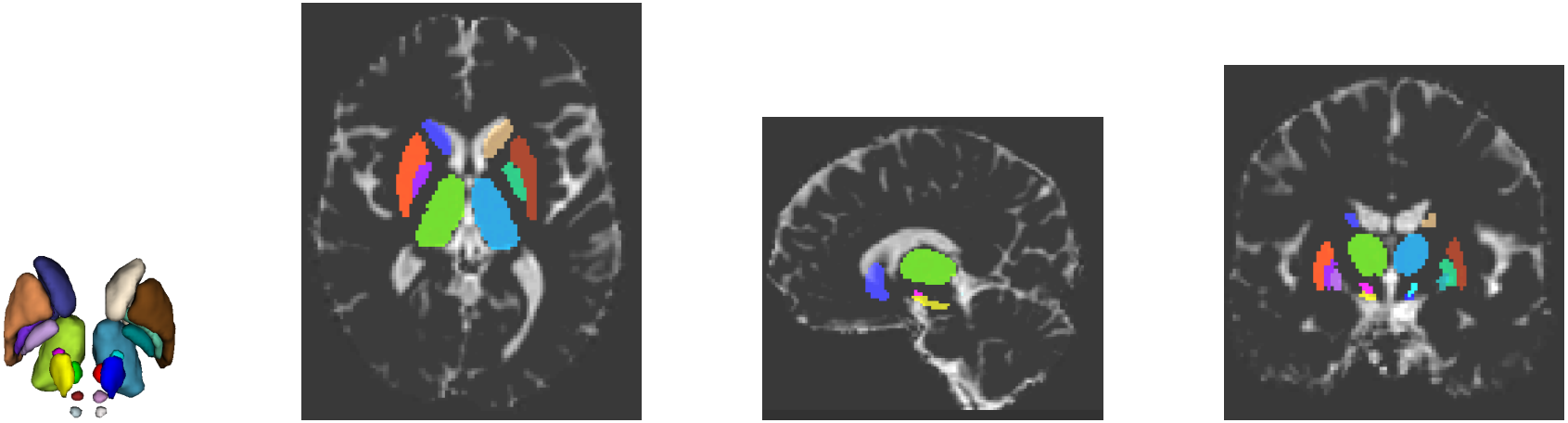

Figure 11: 3D representation, axial slice, sagittal slice and coronal slice depicting 10 subcortical structures

Evaluation metric

- For each individual (controls and patients):
  - For each slice x, compute reconstruction error
  - For each ROI, compute average voxel-wise reconstruction error

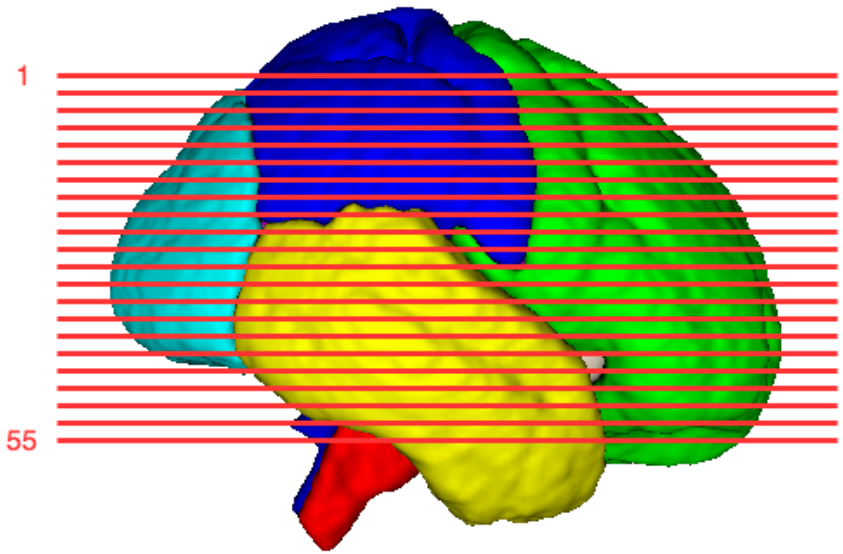

Figure 12: 3D representation of the brain, with 55 axial slices

Evaluation metric

- For each individual (controls and patients):
  - For each slice x, compute reconstruction error
  - For each ROI, compute average voxel-wise reconstruction error

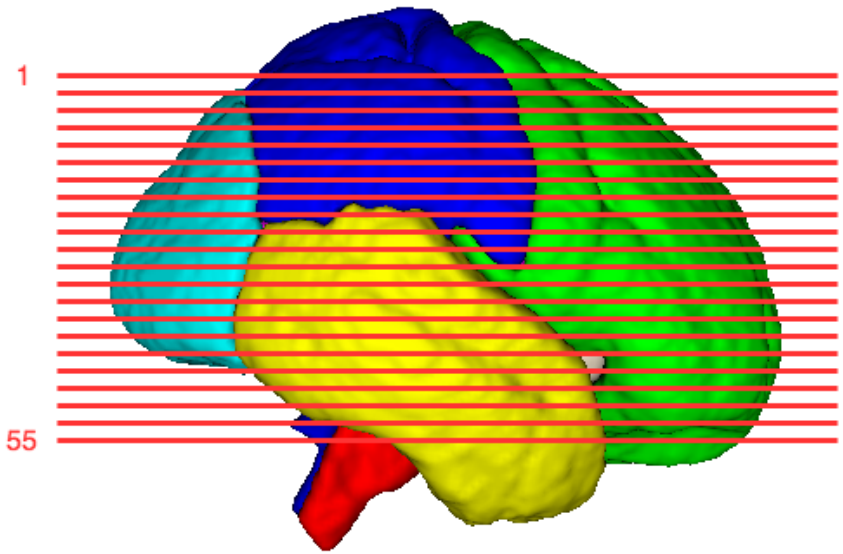

Figure 12: 3D representation of the brain, with 55 axial slices

- For each ROI:
  - Build histogram with average voxel-wise reconstruction errors
  - Build receiver operating characteristic (ROC) curve

Histogram and ROC curve

Example of **sAE** model, **white matter** ROI

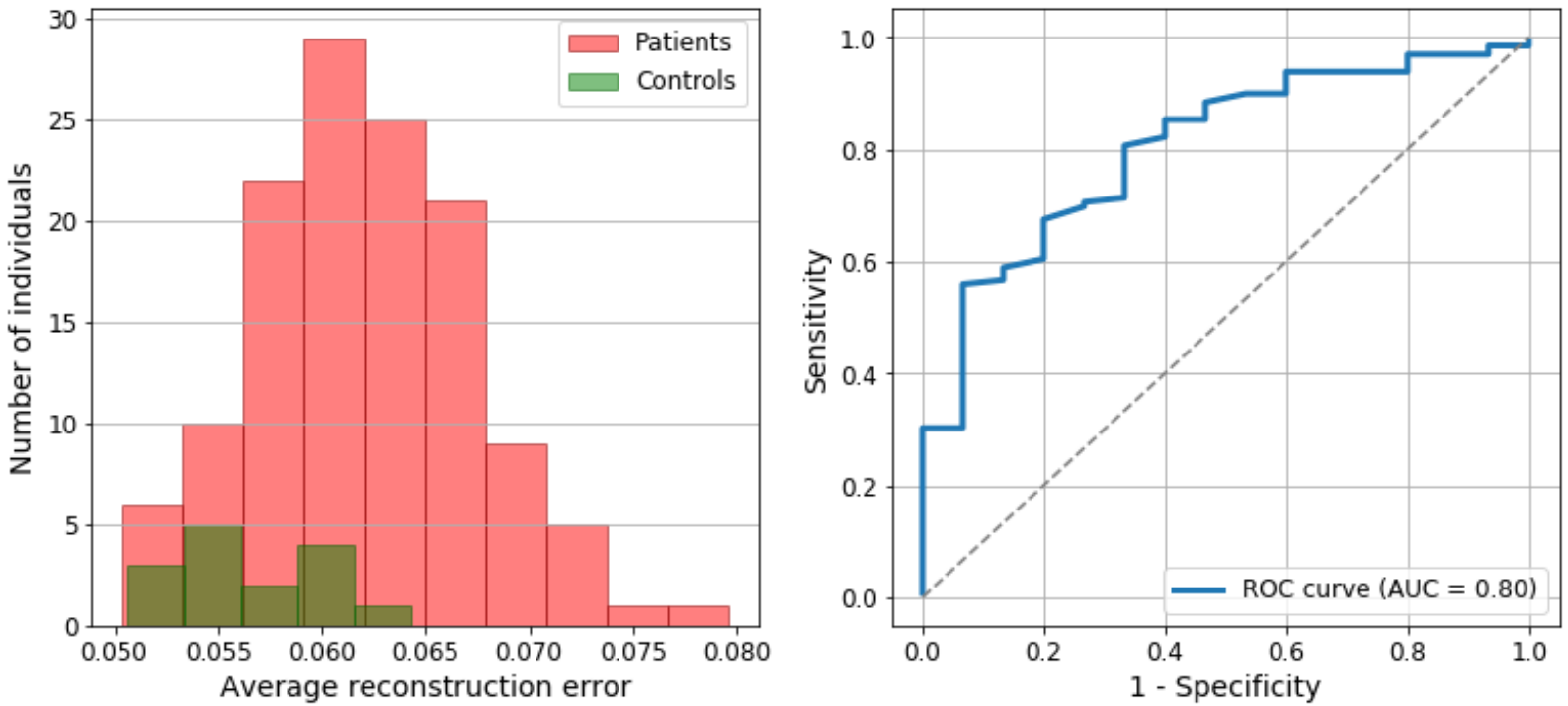

Figure 13: Example of histogram of average pixel-wise reconstruction errors of 15 controls and 129 patients (left) and corresponding ROC curve (right)

Main experiments and results

	U-Net	sAE	sVAE	dVAE
Subcortical structures/Brainstem	**0.70**	**0.76**	**0.77**	**0.70**
Frontal lobe	0.56	0.58	0.56	0.59
Parietal lobe	0.45	0.62	0.62	0.62
Temporal lobe	0.59	0.67	**0.72**	0.69
Occipital lobe	0.35	0.43	0.41	0.43
White matter	0.62	**0.80**	**0.78**	**0.76**
Insular/Cingulate cortex	**0.70**	0.68	**0.76**	0.68
Ventricles	0.68	0.53	0.50	0.52

Table 1: ROC AUC for eight regions of the brain

Main experiments and results

	U-Net	sAE	sVAE	dVAE
Subcortical structures/Brainstem	**0.70**	**0.76**	**0.77**	**0.70**
Frontal lobe	0.56	0.58	0.56	0.59
Parietal lobe	0.45	0.62	0.62	0.62
Temporal lobe	0.59	0.67	**0.72**	0.69
Occipital lobe	0.35	0.43	0.41	0.43
White matter	0.62	**0.80**	**0.78**	**0.76**
Insular/Cingulate cortex	**0.70**	0.68	**0.76**	0.68
Ventricles	0.68	0.53	0.50	0.52

Table 1: ROC AUC for eight regions of the brain

	U-Net	sAE	sVAE	dVAE
Red Nucleus	0.51	0.69	0.64	0.58
Substantia Nigra	0.61	**0.73**	**0.72**	0.66
Subthalamic Nucleus	0.67	0.69	0.66	0.50
Caudate	0.60	0.57	0.53	0.62
Putamen	0.46	0.62	0.61	0.60
Globus Pallidus external	0.54	0.56	0.58	0.60
Globus Pallidus internal	0.54	0.64	0.67	0.64
Thalamus	0.67	0.65	**0.73**	0.68
Superior Colliculus	0.66	0.45	0.54	0.52
Inferior Colliculus	0.55	0.40	0.42	0.43

Table 2: ROC AUC for ten subcortical structures of the brain

Table of Contents

Conclusion

Main findings

- Deep learning models are useful to locate PD related anomalies
  - Most affected: white matter and subcortical structures, consistent with [Taylor et al., 2018, Muñoz Ramírez et al., 2019]
- Fully convolutional networks enable better anomaly detection
  - sAE & sVAE: agreed and performed better

Conclusion

Main findings

- Deep learning models are useful to locate PD related anomalies
  - Most affected: white matter and subcortical structures, consistent with [Taylor et al., 2018, Muñoz Ramírez et al., 2019]
- Fully convolutional networks enable better anomaly detection
  - sAE & sVAE: agreed and performed better

Importance

Help in the quest for robust markers of PD

Conclusion

Main findings

- Deep learning models are useful to locate PD related anomalies
  - Most affected: white matter and subcortical structures, consistent with [Taylor et al., 2018, Muñoz Ramírez et al., 2019]
- Fully convolutional networks enable better anomaly detection
  - sAE & sVAE: agreed and performed better

Importance

Help in the quest for robust markers of PD

Perspectives

- Different architectures (e.g. adding adversarial component)
- Larger cohorts
- More MRI parameters
- Other disorders where no voxel-level ground truth is available

References I

[Alex et al., 2017] Alex, V., Safwan K. P., M., Chennamsetty, S. S., and Krishnamurthi, G. (2017).
Generative adversarial networks for brain lesion detection.
In *Proc. SPIE 10133, Medical Imaging 2017*, page 101330G.

[Atkinson-Clement et al., 2017] Atkinson-Clement, C., Pinto, S., Eusebio, A., and Coulon, O. (2017).
Diffusion tensor imaging in Parkinson's disease: Review and meta-analysis.
Neuroimage-Clinical, 16:98–110.

[Baur et al., 2018] Baur, C., Wiestler, B., Albarqouni, S., and Navab, N. (2018).
Deep autoencoding models for unsupervised anomaly segmentation in brain MR images.
CoRR, abs/1804.04488.

[Chen and Konukoglu, 2018] Chen, X. and Konukoglu, E. (2018).
Unsupervised detection of lesions in brain MRI using constrained adversarial auto-encoders.
CoRR, abs/1806.04972.

References II

[Du et al., 2011] Du, G., Lewis, M. M., Styner, M., Shaffer, M. L., Sen, S., Yang, Q. X., and Huang, X. (2011).
Combined R2* and diffusion tensor imaging changes in the substantia nigra in Parkinson's disease.
Mov. Disord., 26(9):1627–1632.

[Goodfellow et al., 2014] Goodfellow, I., Pouget-Abadie, J., Mirza, M., Xu, B., Warde-Farley, D., Ozair, S., Courville, A., and Bengio, Y. (2014).
Generative adversarial nets.
In Ghahramani, Z., Welling, M., Cortes, C., Lawrence, N. D., and Weinberger, K. Q., editors, *Advances in Neural Information Processing Systems 27*, pages 2672–2680. Curran Associates, Inc.

[Kingma and Welling, 2013] Kingma, D. P. and Welling, M. (2013).
Auto-encoding variational bayes.
CoRR, abs/1312.6114.

[Muñoz Ramírez et al., 2019] Muñoz Ramírez, V., Forbes, F., Arbel, J., Arnaud, A., and Dojat, M. (2019).
Quantitative MRI characterization of brain abnormalities in de novo Parkinsonian patients.
In *ISBI 2019 - IEEE International Symposium on Biomedical Imaging*, Proceedings of IEEE International Symposium on Biomedical Imaging, pages 1–4, Venice, Italy.

References III

[Peran et al., 2010] Peran, P., Cherubini, A., Assogna, F., Piras, F., Quattrocchi, C., Peppe, A., Celsis, P., Rascol, O., Demonet, J. F., Stefani, A., Pierantozzi, M., Pontieri, F. E., Caltagirone, C., Spalletta, G., and Sabatini, U. (2010).
Magnetic resonance imaging markers of Parkinson's disease nigrostriatal signature.
Brain, 133(11):3423–3433.

[Ronneberger et al., 2015] Ronneberger, O., Fischer, P., and Brox, T. (2015).
U-net: Convolutional networks for biomedical image segmentation.
CoRR, abs/1505.04597.

[Schlegl et al., 2017] Schlegl, T., Seeböck, P., Waldstein, S. M., Schmidt-Erfurth, U., and Langs, G. (2017).
Unsupervised anomaly detection with generative adversarial networks to guide marker discovery.
CoRR, abs/1703.05921.

[Schwarz et al., 2013] Schwarz, S. T., Abaei, M., Gontu, V., Morgan, P. S., Bajaj, N., and Auer, D. P. (2013).
Diffusion tensor imaging of nigral degeneration in Parkinson's disease: A region-of-interest and voxel-based study at 3 T and systematic review with meta-analysis.
Neuroimage Clin, 3:481–488.

References IV

[Taylor et al., 2018] Taylor, K. I., Sambataro, F., Boess, F., Bertolino, A., and Dukart, J. (2018).
Progressive decline in gray and white matter integrity in de novo parkinson's disease: An analysis of longitudinal parkinson progression markers initiative diffusion tensor imaging data.
Frontiers in aging neuroscience, 10:318–318.

[Vu et al., 2019] Vu, H. S., Ueta, D., Hashimoto, K., Maeno, K., Pranata, S., and Shen, S. M. (2019).
Anomaly Detection with Adversarial Dual Autoencoders.
arXiv e-prints, page arXiv:1902.06924.

[Zimmerer et al., 2018] Zimmerer, D., Petersen, J., Kohl, S. A., and Maier-Hein, K. H. (2018).
A case for the score: Identifying image anomalies using variational autoencoder gradients.
32nd Conference on Neural Information Processing Systems (NeurIPS 2018), Montreal, Canada.